IEEE Robotics and Automation Letters (RAL) paper presented at the
2020 IEEE/RSJ International Conference on Intelligent Robots and Systems (IROS)
October 25-29, 2020, Las Vegas, NV, USA (Virtual)

Shift-Adaptive Estimation of Joint Angle Using Instrumented Brace With Two Stretch Sensors Based on Gaussian Mixture Models*

Ryo Eguchi[1], Brendan Michael[2], Matthew Howard[2], and Masaki Takahashi[3]

Abstract— **Wearable motion sensing in daily life has attracted attention in various disciplines. Especially, stretchable strain sensors have been instrumented into garments (e.g. brace). To estimate joint motions from such sensors, previous studies have modelled relationships between the sensor strains and motion parameters via supervised/semi-supervised learning. However, typically these only model a single relationship assuming the sensor to be located at a specific point on the body. Consequently, they exhibit reduced performance when the strain-parameter relationship varies due to sensor shifts caused by long-term wearing or donning/doffing of braces. This letter presents a shift-adaptive estimation of knee joint angle. First, a brace is instrumented with two stretch sensors placed at different heights. Next, the different strain-angle relationships at varying brace shift positions are learned using Gaussian mixture models (GMMs). The system then estimates the joint angle from the sensor strains through Gaussian mixture regression using a maximum likelihood shift GMM, which is identified by referring to the two strains in a previous 1 s period. Experimental results indicated that the proposed method estimates the joint angle at multiple shift positions (0–20 mm) with higher accuracy than methods using a single model, single sensor, or referring to the present sensor strains.**

I. INTRODUCTION

Wearable sensing for the tracking and monitoring of human motion has recently attracted attention in various disciplines, including medicine and healthcare [1]–[3], sports science [4]–[6], and human-computer interaction (e.g., virtual/augmented reality [7], [8]). For example, in the field of medicine and healthcare, assessing the kinematic gait parameters such as the range of joint motion yields beneficial information for tracking disease progression and evaluating the effect of clinical interventions (e.g., rehabilitation) of patients with musculoskeletal disorders [9]–[11].

Inertial measurement units (IMUs) integrating accelerometers, gyroscopes, and magnetometers have achieved remarkable development as wearable motion-sensing technologies through advancements in electronic miniaturisation, signal processing, and cost diminishment [12]. Such system reconstructs the motion using the orientations of the IMUs attached to the body segments. For the orientation estimation, a strap-down-integration of the angular rates and a drift elimination using the gravitational acceleration and heading determined from magnetometer measurements are typically employed. Although many sensor fusion algorithms have been proposed, drift elimination in long-term measurements and compensation for magnetic disturbances inevitable in a living environment are still attracting the interest of numerous research groups [13]. In addition, IMUs are typically made of rigid components and must be tightly attached to the body because the motion reconstruction is based on fixed sensor-to-segment frames and linked rigid-body modelling. The restraints these introduce restrict their long-term wearability in daily life.

As alternatives to IMUs, it has been proposed to use wearable sensors that directly measure the changes in the joint angles, such as electrogoniometers (rotational potentiometers) [14], [15], flex sensors [16]–[18], fibre-optic sensors [19]–[22], and stretchable strain sensors [23]–[29]. In particular, the stretch sensor, which transduces a mechanical deformation (sensor strain) to resistive or capacitive change, can (i) comply with fabric stretch and capture motion, (ii) avoid mechanical damage to the sensor, (iii) maintain user comfort when incorporated into garments, such as gloves [25], braces [26], or soft sensing suits [23], [28], [29].

To estimate joint motions from such sensors, previous studies have modelled relationships between the sensor strains and motion parameters (e.g. angles or positions) via supervised/semi-supervised learning. However, typically these only model a single relationship assuming the sensor to be located at a specific point on the body. Consequently, these approaches may exhibit reduced performance when the strain-parameter relationship varies due to shifting of the sensor with respect to the body, which is caused by long-term wearing or donning/doffing of garments. Especially in the brace, Brouwstein [30] reported that 15 min of exercise induces the brace shift of up to 11 mm, and Singer et al. [31] mentioned that individuals will likely stop their activity to adjust the brace position when it has shifted by more than 20 mm distally on the leg. Thus, the previous single model-based approaches may estimate the motion with low accuracy when unnoticed brace shift occurs during long-term use.

To address this, this letter presents a *shift-adaptive estimation* of the knee joint angle. The key contribution is the combination of the following to realise accurate estimation. First, a brace is instrumented with two stretch sensors placed at different heights. The relationship between the two sensor strains varies depending on the brace shift position. Second, the different strain-angle relationships at

This work was supported by JSPS KAKENHI Grant Number JP16H04290, JP19J12205, and JSPS Overseas Challenge Program for Young Researchers.

[1]Ryo Eguchi is with the School of Science for Open and Environmental Systems, Graduate School of Science and Technology, Keio University, Yokohama 223-8522, Japan eguchi.ryo@keio.jp

[2]Brendan Michael and Matthew Howard are with the Centre for Robotics Research, Department of Engineering, King's College London, London WC2R 2LS, UK matthew.j.howard@kcl.ac.uk

[3]Masaki Takahashi is with the Department of System Design Engineering, Faculty of Science and Technology, Keio University, Yokohama 223-8522, Japan takahashi@sd.keio.ac.jp

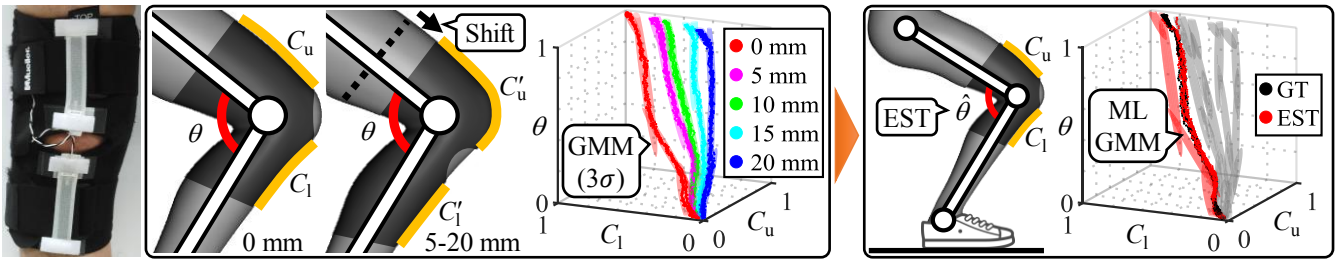

Fig. 1. (a) A wrap-style brace is instrumented with two stretch sensors placed above and below the patella hole. (b) The capacitance (proportional to the sensor strain) decreases more significantly in the lower sensor than the upper sensor ($|C_\mathrm{l} - C'_\mathrm{l}| > |C_\mathrm{u} - C'_\mathrm{u}|$) at the same joint angle when the brace shifts downward. Consequently, the relationship between the two sensor capacitances and the joint angle varies depending on the brace shift position. The system learns these different capacitance-angle relationships at varying brace shift positions using user-specific GMMs. (c) The system estimates the joint angle adaptively to the brace shift through Gaussian mixture regression by identifying a maximum likelihood (ML) shift GMM. In practical use, the learning scheme is applied only once at a clinic, and the system then estimates the joint angle without relearning in daily life.

varying shift positions (every 5 mm from 0 to 20 mm) are learned using Gaussian mixture models (GMMs). Finally, the system estimates the joint angle from the two sensor strains through Gaussian mixture regression. The estimation uses a maximum likelihood shift GMM identified by referring to the relationships between the two sensor strains in a previous 1 s period. This aims at avoiding incorrect identification and frequent switching of the maximum likelihood shift GMM due to the proximity of the learned GMMs and noise of the sensors.

II. RELATED WORKS

For estimating joint motions from the stretch sensors instrumented into garments, previous studies have modelled a relationship between the sensor strains and motion parameters using supervised/semi-supervised learning techniques.

Nakamoto et al. [25] constructed a glove instrumented with a capacitive stretch sensor, whose capacitance was proportional to the square of the stretch length. They applied a linear least-squares technique and estimated the wrist joint angle from the sensor with a root mean square error (RMSE) less than 3°. Totaro et al. [26] integrated three/five capacitive sensors into commercial knee/ankle braces. They then combined sensor outputs using a third, fourth, and fifth-order polynomials and estimated the angles of the knee flexion/extension, ankle dorsi/plantar flexion, adduction/abduction, and rotation with high accuracy (at an RMSE of less than 4°).

As other approaches, Kim et al. [28] modelled the high nonlinearity and hysteresis of soft microfluidic resistive sensors as temporal sequences using a recurrent long short-term memory (LSTM) neural network. The authors predicted full-body joint positions in a three-dimensional space from a soft sensing suit instrumented with 20 stretch sensors. In addition, to reduce both the size and number of the calibration datasets required, they generated lower-limb joint motions from two soft sensors attached to each thigh, based on semi-supervised learning consisting of a deep autoencoder (AE) and a gated recurrent unit (GRU) [29]. The AE embeds the joint positions during gait into a latent motion manifold, and the GRU reduces the computational complexity while maintaining the performance of the LSTM. The RMSE of the estimated terminal joint (toe) position is 30.53 mm.

As described above, there have been numerous studies modelling the relationship between stretch sensor strains and joint motion parameters using machine learning techniques, such as linear/polynomial regressions or deep neural networks (DNN). However, most of them have modelled a single strain-parameter relationship at the appropriate position of the sensors and not supposed that the relationship varies due to sensor shifts. Although a recalibration procedure using a smartphone with a customised application was proposed in [26], users may not notice sensor shifts and not execute recalibration until the shift becomes much more than 20 mm distally on the leg [31]. In addition, DNN may induce larger computational cost/complexity to learn a model, which is adaptive to sensor shifts and corresponds to noncyclic motion. Therefore, for continuous motion sensing in daily life, the sensorised garments are required to identify their own shifts by referring to the sensor strains and estimate motion parameters adaptively to the shifts by changing the model in accordance with the sensor position.

III. METHODS

The flow of the shift-adaptive estimation of the knee joint angle is shown in Fig. 1. At a clinic, a user wears the instrumented brace on the knee and measures joint motions (e.g., squatting) in synchronisation with a ground truth device (e.g., motion capture cameras or IMUs). The different capacitance-angle relationships at varying shift positions are then learned using user-specific GMMs. In daily life, the system estimates the joint angle adaptively to the brace shift using the GMMs without relearning.

A. Instrumented Knee Brace With Two Stretch Sensors

An instrumented brace measuring the knee flexion/extension angle was developed as shown in Fig. 1(a). Flexion/extension occurs along the main axis of the knee motion and is informative for monitoring a progressive gait disorder (e.g., knee osteoarthritis [11]) in daily life. We used a commercial wrap-style brace (Open Patella Knee Stabilizer, Mueller Sports Medicine, Wisconsin, US) aiming for a daily use sensorised treatment device. This type of brace is easily

donned/doffed, adjustable to achieve a comfortable restraint, and effective for the treatment of disorders associated with degenerative cartilage by stabilising the patella [32].

Two electro capacitive stretch sensors (C-STRETCH®, Bando Chemical Industries, Kobe, JP) were placed above and below the patella hole of the brace. The capacitance of the sensor is proportional to the sensor strain. The sensor installation is aimed at recognising brace shifts by referring to the relationship between the two sensor strains while avoiding artefacts from the physical contact of the sensors and the skin. The mechanism of changes in the relationship is illustrated in Fig. 1(b). The capacitance decreases more significantly in the lower sensor than the upper sensor at the same joint angle when the brace shifts downward. This is due to the fact that the fabric of the brace deforms along with the strain in the skin, which are high in the patella area and rapidly decrease away from this region [33].

B. Learning User-specific GMMs from Multiple Brace Shifts

The learning flow of user-specific GMMs is shown in Fig. 1(b). First, a user wears the instrumented brace at the appropriate position on the knee (brace shift of 0 mm). Next, the user performs joint motions including knee flexion/extension (e.g., squatting) with the maximum viable range. The motions are measured by the brace in synchronisation with the ground truth device. The measurement provides a dataset $z \in \mathbb{R}^3$ consisting of the capacitance of the two stretch sensors $x \in \mathbb{R}^2$ and the ground truth of the joint angle $y \in \mathbb{R}$. A GMM of K components is then fitted to the dataset z using the iterative expectation-maximisation (EM) algorithm with k-means clustering. The model is defined based on the following probability density function:

$$p(z) = \sum_{k=1}^{K} \pi_k N(z|\mu_k, \Sigma_k), \quad \sum_{k=1}^{K} \pi_k = 1 \tag{1}$$

where π_k indicates the prior probabilities and $N(z|\mu_k, \Sigma_k)$ are the Gaussian distributions defined by the mean vectors μ_k and covariance matrices Σ_k, whose components can be represented separately as follows:

$$\mu_k = \begin{bmatrix} \mu_{x,k} & \mu_{y,k} \end{bmatrix}, \quad \Sigma_k = \begin{pmatrix} \Sigma_{xx,k} & \Sigma_{xy,k} \\ \Sigma_{yx,k} & \Sigma_{yy,k} \end{pmatrix} \tag{2}$$

Following collecting data at zero shift, the brace is migrated to varying anticipated shift positions (every 5 mm up to 20 mm in this study). The knee flexion/extension angle is then measured during the same joint motion, and a GMM is fitted to the dataset of each shift position. Finally, the GMMs at all shifts are integrated with equal mixing proportions. Note that although increasing the number of considered brace shift position may enhance the performance of the system, it requires a larger computational cost for learning and increases the physical burden on users.

C. Shift-adaptive Estimation of Knee Joint Angle

The system estimates the joint angle from the two sensor capacitances according to brace shifts, by identifying the maximum likelihood (ML) shift GMM from the integrated GMMs. Although the identification typically refers to the present sensor capacitances, the measurement error and sensor noise may induce incorrect identification or frequent switching when the relationships in two sensor capacitances between the shift GMMs are proximate. Therefore, we propose to identify the ML shift GMM by referring to the two sensor capacitances within a fixed time window.

When given the capacitance of the two sensors x, the probability of each component k of the integrated GMMs is defined as follows:

$$\beta_k = \frac{p(k)\, p(x|k)}{\sum_{i=1}^{nK} p(i)\, p(x|i)} = \frac{\pi_k p\left(x \middle| \mu_{x,k}, \Sigma_{xx,k}\right)}{\sum_{i=1}^{nK} \pi_i p\left(x \middle| \mu_{x,i}, \Sigma_{xx,i}\right)} \tag{3}$$

where n is the number of learned shift GMMs (five in this study). Using β_k, the system identifies the ML shift GMM by referring to the summed probabilities of K components of each shift GMM averaged in a certain time window T as follows:

$$\begin{gathered} \arg\max_m \frac{1}{T} \sum_{t=t_0-T}^{t_0} \sum_{k=1}^{K} \beta_{k,m} \\ m = \{1, 2, ..., n\}, \ \hat{\theta}(t) < \theta_{ub} \end{gathered} \tag{4}$$

where t_0 is the last frame and m is the ML shift GMM. The time window T includes only frames in which the estimated joint angle is lower than θ_{ub}. This condition aims to exclude datasets of larger joint angles when the sensor stretches are close to maximum, in which capacitances of the shift GMMs are proximate despite their differing angles.

Using the identified ML shift GMM, the system estimates the joint angle from the present two sensor capacitances through Gaussian mixture regression (GMR) [34].

IV. EXPERIMENT

A. Setup

Two healthy adults (male, age: 26±1 years, height: 1.78±0.5 m, body mass: 64.5±2.5 kg) participated in this study. Ethical approval was obtained from Keio University Research Ethics Committee (reference number 31–80) and informed consent was provided by the participants prior to the experiments. The participants wore the instrumented brace on the right knee at a comfortable tightness. Hard thin CEM-3 plates (95 × 72 × 1.6 mm) incorporating three infrared reflective markers were then tightly attached to the right thigh and shank. The positions of the plates were chosen such that upper/lower markers on the thigh/shank were located along a line connecting the greater trochanter and the ankle joint. The capacitance of the two stretch sensors was amplified and DA-converted using a dedicated module (KIT BT01, Bando Chemical Industries, Hyogo, JP) placed on the brace. A data logger (TSND151, ATR Promotions, Kyoto, JP) on the thigh plate then AD-converted the voltage outputs of the module and transmitted them to a laptop computer at 200 Hz through Bluetooth communication. Additional markers sets were attached to the front of the thigh and shank and the upper/lower edges of the brace for measuring the distances of brace shifts. Landmark stickers representing a 5 mm spacing from 0 to 20 mm also adhered to the thigh

and shank for manual brace shifting. The positions of the reflective markers on the thigh and shank were obtained by a motion capture system (Nexus, Vicon, Oxford, UK) at 100 Hz. All devices were synchronised using a voltage input.

B. Virtual Knee Joint Marker Generation

The ground truth of the knee joint angle can be calculated as the angle between two vectors from the knee joint to the greater trochanter and the ankle joint. However, a reflective marker could not be attached to the knee joint directly because the participants wore the knee brace and shifted it during the experiment. Therefore, a virtual knee joint marker was generated by referring to the positions of three markers on the plates attached to the thigh and shank, which could be modelled as rigid body segments.

The marker generation was executed through an optimisation inspired by a gap-filling algorithm [35]. The algorithm fills a target marker unobservable at an interpolation frame t_i by using the positions of the target marker observable at a reference frame t_r and a rotation matrix of three reference markers from t_r to t_i. At the reference frame t_r and the interpolation frame t_i, the relative positions of the reference markers $\mathrm{M}(t_{r/i})$ to their center $\mathrm{O}(t_{r/i})$ is defined as follows:

$$\bar{\mathrm{M}}(t_{r/i}) = \mathrm{M}(t_{r/i}) - \mathrm{O}(t_{r/i}) = \mathrm{M}(t_{r/i}) - \frac{1}{3}\sum_{j=1}^{3}\mathrm{M}_j(t_{r/i}) \quad (5)$$

A rotation matrix R from t_r to t_i can be generated by calculating a covariance matrix C and by applying a singular value decomposition using the Kabsch algorithm as follows:

$$\mathrm{C} = \bar{\mathrm{M}}(t_r)^{\mathsf{T}}\bar{\mathrm{M}}(t_i) = \mathrm{USV}^{\mathsf{T}} \quad (6)$$

$$\mathrm{R}(t_i) = \mathrm{V}\begin{bmatrix} 1 & 0 & 0 \\ 0 & 1 & 0 \\ 0 & 0 & d \end{bmatrix}\mathrm{U}^{\mathsf{T}},\ d = \begin{cases} -1 & (\det(\mathrm{VU}^{\mathsf{T}}) < 0) \\ 1 & (otherwise) \end{cases} \quad (7)$$

The target marker positions at t_i are then calculated using the rotation matrix R, the relative positions of the target marker at the reference frame $\bar{\mathrm{P}}(t_r)$, and $\mathrm{O}(t_i)$.

$$\begin{aligned} \mathrm{P}(t_i) &= \mathrm{R}(t_i)\bar{\mathrm{P}}(t_r) + \mathrm{O}(t_i) \\ &= \mathrm{R}(t_i)\{\mathrm{P}(t_r) - \mathrm{O}(t_r)\} + \mathrm{O}(t_i) \end{aligned} \quad (8)$$

Based on the above algorithm, we identified the virtual knee joint marker positions $\mathrm{P}(t_r)$ through a nonlinear optimisation minimising the sum of the following two distances during knee flexion/extension. One was the error between the two virtual marker positions estimated from three reference markers on the thigh and shank, respectively, and the other was the distance from the upper marker on the thigh to the lower marker on the shank through the virtual marker (meaning all markers should be on the same plane). The optimisation is defined as follows:

$$\min_x \|f(x)\|_2^2 = \min_x \left(f_1(x)^2 + f_2(x)^2 + \ldots + f_n(x)^2\right) \quad (9)$$

$$\begin{aligned} f(\mathrm{P}(t_r)) =& \{\mathrm{R}_t(t_i)\{\mathrm{P}(t_r) - \mathrm{O}_t(t_r)\} + \mathrm{O}_t(t_i)\} \\ &- \{\mathrm{R}_s(t_i)\{\mathrm{P}(t_r) - \mathrm{O}_s(t_r)\} + \mathrm{O}_s(t_i)\} \\ &+ \{\mathrm{P}(t_r) - \mathrm{O}_t(t_r)\} + \{\mathrm{P}(t_r) - \mathrm{O}_s(t_r)\} \end{aligned} \quad (10)$$

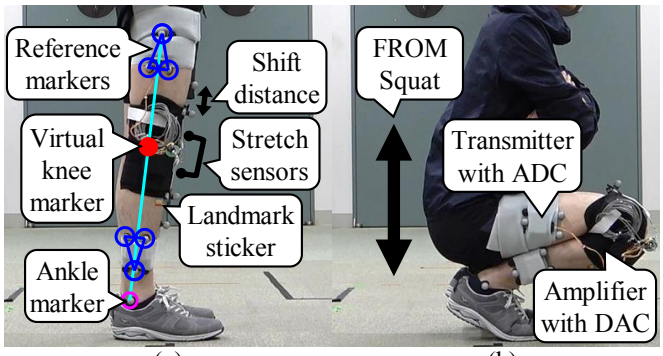

Fig. 2. The participants were asked to perform two motions for each brace shift position. (a) Standing still for measuring brace shift distances. (b) FROM squat for generating a virtual knee joint marker shown in (a) and learning and testing the estimation methods.

C. Study Procedure

For validating the proposed shift-adaptive estimation method, the participants were asked to perform the following tasks:

A) For generating the virtual knee joint marker as shown in Fig. 2(a), the participants performed a full range of motion (FROM) squat five times during a 20 s period at the beginning of the experiment.
B) For measuring the brace position, the participants stood still for 10 s while wearing the brace at the non-shift position, as shown in Fig. 2(a).
C) For learning and testing the estimation method, the participants performed a FROM squat five times within a 40 s period, as shown in Fig. 2(b). During this motion, they took a 2-s rest after every squat-stand motion.
D) The participants migrated the brace manually to the anticipated shift positions (5, 10, 15, and 20 mm away from the initial position) according to the landmark stickers. They then repeated tasks B and C for each brace shift position.
E) The participants returned the brace to the initial position and performed tasks B–D once more to reenact donning/doffing or position correction of the brace.

Tasks B–E indicate that standing still and the FROM squats were measured for two sets of brace shifts (every 5 mm from 0 to 20 mm) in total.

D. Acquisition of Brace Shift Distance

The brace shift distance at each shift position was calculated as the mean distance between markers on the front of the thigh/shank and on the upper/lower edges of the brace during standing still for tasks B, D and E.

E. Preparation of Learning and Testing Datasets

Using the marker positions obtained in task A, the virtual knee joint marker was generated through the optimisation (9), (10) using MATLAB (MathWorks, Natick, MA, US) Optimization Toolbox (lsqnonlin). The knee joint angle during the squat for tasks C–E was then calculated as the angle between two vectors, which are from the virtual knee joint marker,

generated by referring to the markers sets on the shank, to the upper reference marker on the thigh and the ankle marker. The AD-converted capacitances of the two stretch sensors were filtered by moving average with a time window of 20 ms for reducing noise and then resampled at 100 Hz to match the motion capture system.

The data sets consisting of the two sensor capacitances and the joint angle during the squat were then divided into the knee flexion (including rest) and extension motions by referring to the plus/minus sign of the derivative capacitance in the upper stretch sensor. This was aimed at modelling the capacitance-angle relationships, which differ between the stretch and relaxation owing to the different delay times for the capacitance-to-voltage conversion of the amplifier. The numerical differentiation was executed using the first-order derivatives and a moving average filter with a time window of 200 ms. Note that this operation will likely be unnecessary in the future if an improvement in the processing speed of the amplifier can be achieved. All datasets were scaled to [0, 1] by referring to the measurement range for both sets of brace shifts, and then homogenised using a box grid filter.

F. Training and Test of Proposed/comparative Methods

Datasets of each set of brace shifts (every 5 mm from 0 to 20 mm) were used for training, and datasets of the other set were used for testing for cross-validation. For training, user-specific GMMs were fitted to the datasets of the five brace shift positions. The number of GMM components was set to five such that the AIC and BIC values were sufficiently small. For testing, the proposed method estimated the joint angle of the datasets of each set by using the GMMs trained using the other set. As described in section III.C, the ML shift GMM was identified by referring to the average probability of each shift GMM in a certain previous period of time. The time window T was set to 1 s, and the upper limit of data used for the identification was set to $\theta_{ub} = 140°$. Using the identified ML shift GMM, the joint angle was estimated from the present two sensor capacitances through GMR. The first round of the squat was excluded from the test section as a sufficient period of time for identifying the first ML shift GMM.

To assess the advantages of the proposed method using the previous ML shift model (PV), three comparative methods using the same datasets for learning and testing were examined as follows:

- Single Model (SM): The method learns the relationship between the two sensor capacitances and the joint angle at non-shift (0 mm) position as a single GMM.
- Single Sensor (SS): The method learns the relationships between only the upper sensor capacitance and the joint angle at five shift positions. The joint angle is estimated using the ML shift GMM identified by referring only to upper sensor capacitance.
- Present ML Model (PS): The method learns the relationships between the two sensor capacitances and the joint angle at five shift positions similar to PV. The joint angle is estimated using the ML shift GMM identified by referring to the present two sensor capacitances.

The effectivenesses of the multiple shift models, multiple sensors, and the ML shift GMM in a 1 s window are assessed through comparisons between SM–PS, SS–PS, and PS–PV, respectively.

TABLE I

BRACE SHIFTS AND ERROR IN ESTIMATED JOINT ANGLES.

Sub (Set)	Brace shift (mm) Target	Measured	RMSE of estimated joint angle (°) SM	SS	PS	PV
A (1st)	0	-	**3.7**	4.5	**3.7**	**3.7**
	5	8.8	6.3	6.7	5.9	**4.7**
	10	13.2	10.3	7.4	**3.2**	4.2
	15	17.6	15.0	5.8	4.4	**4.2**
	20	26.9	23.6	9.7	10.5	**4.0**
	Overall		11.8±7.9	6.8±1.9	5.6±2.9	**4.2±0.4**
A (2nd)	0	2.9	**2.7**	4.6	5.0	3.1
	5	10.3	19.6	4.3	**2.7**	3.2
	10	18.0	36.0	4.9	4.1	**3.9**
	15	19.1	39.3	6.3	5.4	**3.5**
	20	29.9	23.9	9.3	4.0	**3.7**
	Overall		24.3±14.6	5.9±2.0	4.2±1.1	**3.5±0.3**
B (1st)	0	-	10.4	7.6	6.1	**5.8**
	5	1.3	5.9	7.7	5.3	**4.8**
	10	6.9	6.6	6.0	3.9	**3.2**
	15	12.4	12.7	5.8	5.7	**3.1**
	20	18.2	17.0	8.3	**3.3**	3.4
	Overall		10.5±4.6	7.1±1.1	4.9±1.2	**4.1±1.2**
B (2nd)	0	0.0	7.8	7.6	6.7	**6.5**
	5	2.5	7.6	7.5	**5.9**	6.7
	10	6.2	6.1	6.7	3.5	**2.8**
	15	10.3	4.7	6.7	2.9	**2.8**
	20	19.4	7.0	7.2	3.0	**2.9**
	Overall		6.6±1.3	7.1±0.4	4.4±1.8	**4.3±2.1**

V. RESULTS

The relationships between the normalised capacitances of the two stretch sensors and the joint angle during a knee extension at five brace shift positions, the same datasets plotted into each 2-D space, and the fitted GMMs are illustrated in Fig. 3. The measured brace shift distances and the accuracies of the joint angles estimated by comparative and proposed methods during the squat motion are listed in Table I. The method with the best performance at each shift position is highlighted in bold. The joint angles estimated by SS, PS, and PV, their absolute error, and ML shift models identified during two rounds of the squat motion are shown in Fig. 4. The results are for two brace shift positions (5 and 20 mm) of the first set for both subjects.

VI. DISCUSSION

In this study, we proposed the shift-adaptive estimation of the knee joint angle by combining the following: (i) a brace instrumented with two stretch sensors placed at different heights, (ii) learning the strain-angle relationships at multiple brace shift positions through user-specific GMMs, and (iii) estimation using an ML shift GMM in a previous 1 s period.

As illustrated in Fig. 3, the relationship between the two sensor capacitances and the joint angle varies depending on the brace shift position. More specifically, the capacitance-angle relationship for each sensor changes according to

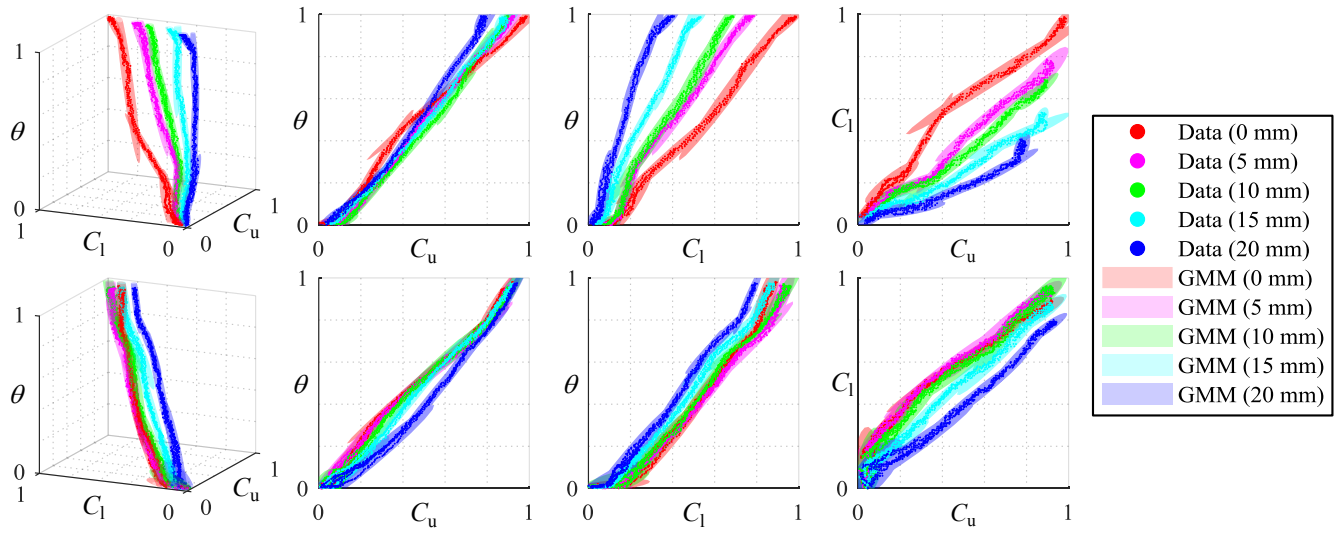

Fig. 3. Relationships between the normalised capacitances of the two stretch sensors (C_u,C_l) and the joint angle θ, the same datasets plotted into each 2-D space, and the fitted GMMs ($\pm 3\sigma$) during knee extension at five brace shifts (0–20 mm) of the second set for both subject A (top) and B (bottom).

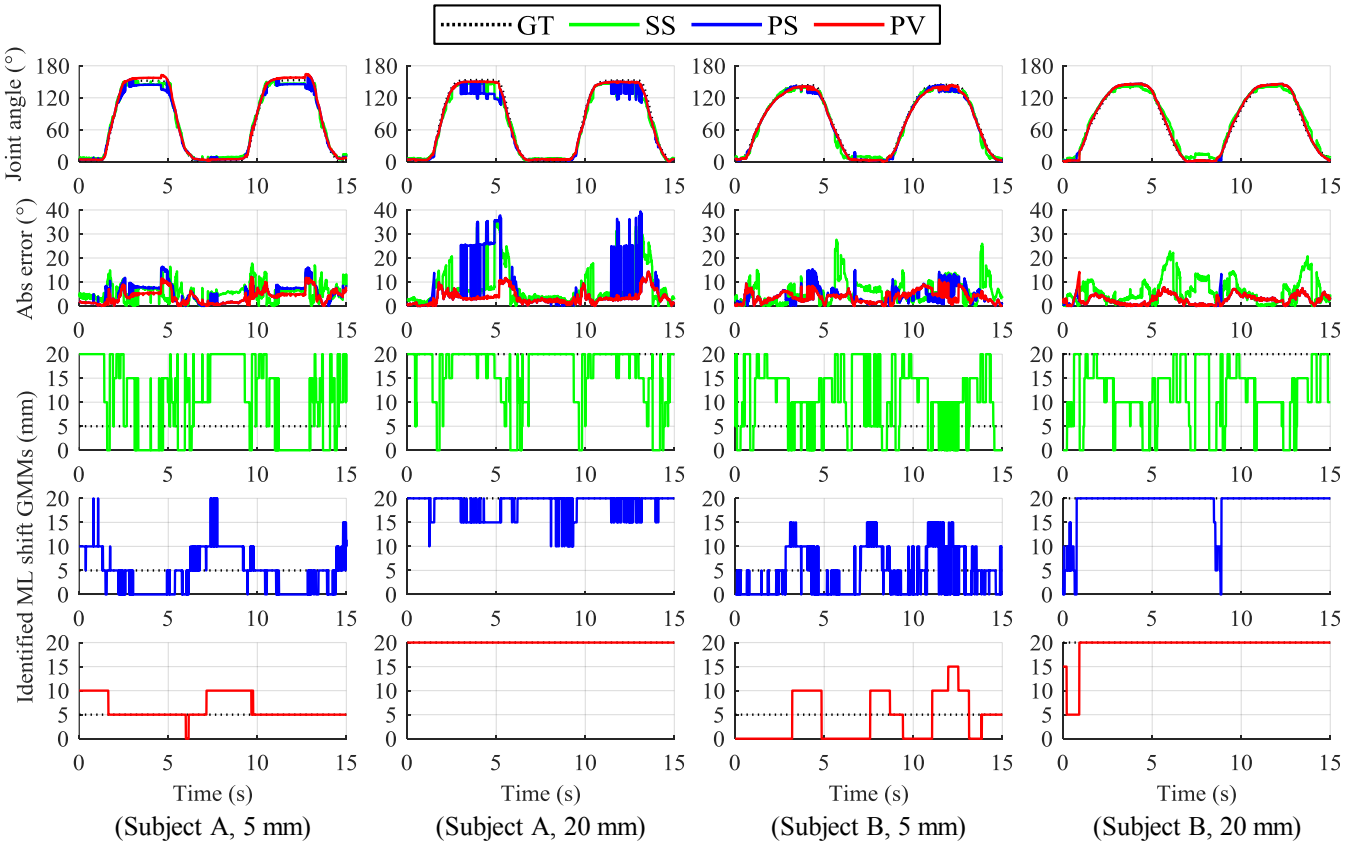

Fig. 4. Ground truth (GT) of the joint angles and estimates of the comparative and proposed methods (SS, PS, PV) (top), their absolute error (the second row), and ML shift GMMs identified by each method during two rounds of the squat motion (the lower three). The results are for two brace shift positions (5 and 20 mm) of the first set for both subjects.

the brace shift, and more significant change in the lower sensor induces different relationships between the two sensor capacitances at varying shift positions. In addition, as indicated in Table I, SM has low accuracy at all brace shifts except for 0 mm of subject A when compared with PS. These results demonstrated that learning the strain-angle relationships at multiple brace shift positions is required for the shift-adaptive estimation.

Table I also shows that SS had a lower accuracy at most brace shifts when compared with PS. As shown in Fig. 4, SS did not identify the correct ML shift GMM according to the brace shift even at larger joint angles, in which the relationship between two sensor capacitances differed clearly between GMMs in Fig. 3. These results demonstrated that the two sensors placed above and below the patella hole are essential for recognising the brace shift positions to identify the correct GMM.

From Table I, PV exhibited an equivalent or higher performance to that of PS at most shift positions of both sets for both subjects. As shown in Fig. 4, although both PV and PS identified the ML shift GMM according to the brace shift, PS switched the GMM frequently and decreased the accuracy due to incorrect identification of the GMM when the angle was close to the maximum. These results were due to the measurement error and noise of the sensors and the proximity of the capacitances between the GMMs near the maximum flexion angle, as shown in Fig. 3. In contrast to PS, PV achieved higher performance through stable identification of the correct ML shift GMM. These results indicate that identification referring to the two sensor capacitances in a previous 1 s period excluding data near the largest angle enhances the estimation.

From the above results, we found that the proposed method can estimate the joint angle with higher accuracy than previous methods when the brace shifts downward, and the three components are effective for the shift-adaptive estimation.

Meanwhile, there are two limitations to this study. One is that the methods were only tested for two healthy participants. Thus, the results do not provide strong statistical support for the proposed method. However, the cross-validation using individual data is worthwhile since the proposed method learns user-specific models. Although the method is data-driven and its performance depends on training data, the results indicate that the method can identify the correct shift GMM and estimate the joint angle with high accuracy if the brace position is not much away from the positions during learning. As shown in Fig. 3, the relationships between the two sensor capacitances and the joint angle exhibited different tendencies between both participants. These results may be due to the differences in the measured shift distances and tightness of the brace. As shown in Table I, the brace shift distances were larger in subject A and smaller in subject B when compared with the targets because subject B preferred tighter fitting of the brace than subject A. Nevertheless, the finding of this study is that the proposed method can estimate the joint angle adaptively to brace shifts using the ML shift GMM identified by referring to the relationship between the two sensor capacitances, regardless of the tightness of the brace.

The other limitation is the reenactment of the brace shift. In this study, the brace was shifted downward manually because it is difficult to induce the intended quantitative shift during long-term wearing of the brace. Moreover, changes in tightness of the brace due to donning/doffing, which may change the strain-angle relationship, was not examined since this study focused on the adaptation to the brace shift. (Note that the tightness can be kept constant by memorising the wrap length during learning.)

Future work will examine the feasibility of tracking dynamic motion (e.g., walking) continuously and validate the proposed shift-adaptive estimation during long-term wearing and donning/doffing of the brace in daily life. The system will then be expanded to an estimation of three-dimensional joint motions such as the ankle and elbow joints. These sensing systems can also be integrated into a robotic motion assist/support system.

REFERENCES

[1] F. Feldhege, A. Mau-Moeller, T. Lindner, A. Hein, A. Markschies, U. K. Zettl, and R. Bader, "Accuracy of a custom physical activity and knee angle measurement sensor system for patients with neuromuscular disorders and gait abnormalities," *Sensors*, vol. 15, no. 5, pp. 10 734–10 752, 2015.

[2] C. Z.-H. Ma, D. W.-C. Wong, W. K. Lam, A. H.-P. Wan, and W. C.-C. Lee, "Balance improvement effects of biofeedback systems with state-of-the-art wearable sensors: A systematic review," *Sensors*, vol. 16, no. 4, 2016.

[3] A. I. Faisal, S. Majumder, T. Mondal, D. Cowan, S. Naseh, and M. J. Deen, "Monitoring methods of human body joints: State-of-the-art and research challenges," *Sensors*, vol. 19, no. 11, 2019.

[4] V. Camomilla, E. Bergamini, S. Fantozzi, and G. Vannozzi, "Trends supporting the in-field use of wearable inertial sensors for sport performance evaluation: A systematic review," *Sensors*, vol. 18, no. 3, 2018.

[5] G. De Pasquale and V. Ruggeri, "Sensing strategies in wearable biomechanical systems for medicine and sport: a review," *Journal of Micromechanics and Microengineering*, vol. 29, no. 10, p. 103001, 2019.

[6] Y. Adesida, E. Papi, and A. H. McGregor, "Exploring the role of wearable technology in sport kinematics and kinetics: A systematic review," *Sensors*, vol. 19, no. 7, 2019.

[7] A. Karatsidis, R. E. Richards, J. M. Konrath, J. C. van den Noort, H. M. Schepers, G. Bellusci, J. Harlaar, and P. H. Veltink, "Validation of wearable visual feedback for retraining foot progression angle using inertial sensors and an augmented reality headset," *Journal of NeuroEngineering and Rehabilitation*, vol. 15, no. 1, p. 78, 2018.

[8] Y. Lee, M. Kim, Y. Lee, J. Kwon, Y. Park, and D. Lee, "Wearable finger tracking and cutaneous haptic interface with soft sensors for multi-fingered virtual manipulation," *IEEE/ASME Transactions on Mechatronics*, vol. 24, no. 1, pp. 67–77, Feb 2019.

[9] J. L. Astephen, K. J. Deluzio, G. E. Caldwell, and M. J. Dunbar, "Biomechanical changes at the hip, knee, and ankle joints during gait are associated with knee osteoarthritis severity," *Journal of Orthopaedic Research*, vol. 26, no. 3, pp. 332–341, 2008.

[10] D. Bytyqi, B. Shabani, S. Lustig, L. Cheze, N. Karahoda Gjurgjeala, and P. Neyret, "Gait knee kinematic alterations in medial osteoarthritis: three dimensional assessment," *International Orthopaedics*, vol. 38, no. 6, pp. 1191–1198, Jun 2014.

[11] X. Zeng, L. Ma, Z. Lin, W. Huang, Z. Huang, Y. Zhang, and C. Mao, "Relationship between kellgren-lawrence score and 3d kinematic gait analysis of patients with medial knee osteoarthritis using a new gait system," *Scientific Reports*, vol. 7, no. 1, p. 4080, 2017.

[12] C. Wong, Z.-Q. Zhang, B. Lo, and G.-Z. Yang, "Wearable sensing for solid biomechanics: A review," *IEEE Sensors Journal*, vol. 15, no. 5, pp. 2747–2760, 2015.

[13] P. Picerno, "25 years of lower limb joint kinematics by using inertial and magnetic sensors: a review of methodological approaches," *Gait & posture*, vol. 51, pp. 239–246, 2017.

[14] J. L. Riskowski, "Gait and neuromuscular adaptations after using a feedback-based gait monitoring knee brace," *Gait & posture*, vol. 32, no. 2, pp. 242–247, 2010.

[15] S. Pant, S. Umesh, and S. Asokan, "Knee angle measurement device using fiber bragg grating sensor," *IEEE Sensors Journal*, vol. 18, no. 24, pp. 10 034–10 040, Dec 2018.

[16] P. T. Wang, C. E. King, A. H. Do, and Z. Nenadic, "A durable, low-cost electrogoniometer for dynamic measurement of joint trajectories," *Medical engineering & physics*, vol. 33, no. 5, pp. 546–552, 2011.

[17] A. Tognetti, F. Lorussi, N. Carbonaro, and D. De Rossi, "Wearable goniometer and accelerometer sensory fusion for knee joint angle measurement in daily life," *Sensors*, vol. 15, no. 11, pp. 28 435–28 455, 2015.

[18] Z. A. Abro, Z. Yi-Fan, C. Nan-Liang, H. Cheng-Yu, R. A. Lakho, and H. Halepoto, "A novel flex sensor-based flexible smart garment for monitoring body postures," *Journal of Industrial Textiles*, vol. 49, no. 2, pp. 262–274, 2019.

[19] P. T. Gibbs and H. Asada, "Wearable conductive fiber sensors for multi-axis human joint angle measurements," *Journal of NeuroEngineering and Rehabilitation*, vol. 2, no. 1, p. 7, 2005.

[20] D. Z. Stupar, J. S. Bajic, L. M. Manojlovic, M. P. Slankamenac, A. V. Joza, and M. B. Zivanov, "Wearable low-cost system for human joint movements monitoring based on fiber-optic curvature sensor," *IEEE Sensors Journal*, vol. 12, no. 12, pp. 3424–3431, Dec 2012.

[21] A. A. Mohamed, J. Baba, J. Beyea, J. Landry, A. Sexton, and C. A. McGibbon, "Comparison of Strain-Gage and Fiber-Optic Goniometry for Measuring Knee Kinematics During Activities of Daily Living and Exercise," *Journal of Biomechanical Engineering*, vol. 134, no. 8, 08 2012, 084502.

[22] A. Rezende, C. Alves, I. Marques, M. A. Silva, and E. Naves, "Polymer optical fiber goniometer: A new portable, low cost and reliable sensor for joint analysis," *Sensors*, vol. 18, no. 12, 2018.

[23] Y. Mengüç, Y.-L. Park, H. Pei, D. Vogt, P. M. Aubin, E. Winchell, L. Fluke, L. Stirling, R. J. Wood, and C. J. Walsh, "Wearable soft sensing suit for human gait measurement," *The International Journal of Robotics Research*, vol. 33, no. 14, pp. 1748–1764, 2014.

[24] H. Lee, J. Cho, and J. Kim, "Printable skin adhesive stretch sensor for measuring multi-axis human joint angles," in *2016 IEEE International Conference on Robotics and Automation (ICRA)*, May 2016, pp. 4975–4980.

[25] H. Nakamoto, H. Ootaka, M. Tada, I. Hirata, F. Kobayashi, and F. Kojima, "Stretchable strain sensor with anisotropy and application for joint angle measurement," *IEEE Sensors Journal*, vol. 16, no. 10, pp. 3572–3579, May 2016.

[26] M. Totaro, T. Poliero, A. Mondini, C. Lucarotti, G. Cairoli, J. Ortiz, and L. Beccai, "Soft smart garments for lower limb joint position analysis," *Sensors*, vol. 17, no. 10, 2017.

[27] B. Huang, M. Li, T. Mei, D. McCoul, S. Qin, Z. Zhao, and J. Zhao, "Wearable stretch sensors for motion measurement of the wrist joint based on dielectric elastomers," *Sensors*, vol. 17, no. 12, 2017.

[28] D. Kim, J. Kwon, S. Han, Y. Park, and S. Jo, "Deep full-body motion network for a soft wearable motion sensing suit," *IEEE/ASME Transactions on Mechatronics*, vol. 24, no. 1, pp. 56–66, Feb 2019.

[29] D. Kim, M. Kim, J. Kwon, Y. Park, and S. Jo, "Semi-supervised gait generation with two microfluidic soft sensors," *IEEE Robotics and Automation Letters*, vol. 4, no. 3, pp. 2501–2507, July 2019.

[30] B. Brownstein, "Migration and design characteristics of functional knee braces," *Journal of Sport Rehabilitation*, vol. 7, no. 1, pp. 33 – 43, 1998.

[31] J. C. Singer and M. Lamontagne, "The effect of functional knee brace design and hinge misalignment on lower limb joint mechanics," *Clinical Biomechanics*, vol. 23, no. 1, pp. 52 – 59, 2008.

[32] N. A. Wilson, B. T. Mazahery, J. L. Koh, and L.-Q. Zhang, "Effect of bracing on dynamic patellofemoral contact mechanics." *Journal of Rehabilitation Research & Development*, vol. 47, no. 6, 2010.

[33] B. Pierrat, C. Millot, J. Molimard, L. Navarro, P. Calmels, P. Edouard, and S. Avril, "Characterisation of knee brace migration and associated skin deformation during flexion by full-field measurements," *Experimental Mechanics*, vol. 55, no. 2, pp. 349–360, Feb 2015.

[34] A. Billard, S. Calinon, R. Dillmann, and S. Schaal, "Robot programming by demonstration," *Springer handbook of robotics*, pp. 1371–1394, 2008.

[35] Gap filling algorithm: Rigid Body, VICON Support FAQs for software, Vicon Nexus. [Online]. Available: https://www.vicon.com/support/faqs/ (As of Dec 2019)